PAPER

Check for updates

Increasing the limits of energy and safety in tetrazoles: dioximes as unusual precursors to very thermostable and insensitive energetic materials†

Jatinder Singh, [ID] [a] Richard J. Staples [ID] [b] and Jean'ne M. Shreeve [ID] *[a]

Donor–acceptor hydrogen (H)-bonding contributes to good temperature resistance for energetic compounds. Now we report a strategy which maximizes donor–acceptor H-bonding sites in the construction of new energetic compounds. The straightforward synthesis of 1,2-di(1*H*-tetrazol-5-yl) ethane-1,2-dione dioxime (**2**), as an unusual energetic precursor to highly thermostable and insensitive energetic materials was achieved in four steps from glyoxal (40% in water). The oxime group in compound **2** acts as a H-bond donor and acceptor and its salt formation reaction with hydroxylamine maximizes H-bonding interactions. Dihydroxylammonium 1,2-di(1*H*-tetrazol-5-yl) ethane-1,2-dione, **3**, exhibits high thermal stability (285 °C) and insensitivity to impact (>60 J) and friction (>360 N) owing to the presence of donor–acceptor H-bonds and wave-like crystal packing. It has high heat of formation (524.3 kJ mol^{-1}) and high detonation velocity of 9114 ms^{-1}. Compound **3** exhibits high safety, ultrahigh power and good compatibility, which make it a potential high-energy-density material for practical use.

Anniversary statement

At the 1989 Dallas American Chemical Society meeting, we learned that the Royal Society of Chemistry was launching a new materials journal, the *Journal of Materials Chemistry*, in 1991. The wide acceptance of this journal as the place for the world's best materials work necessitated division into three journals providing coverage of the expanding materials field – the first volume of the *Journal of* M*aterial*s Re*search A* appeared in 2013. A paper entitled "Derivatives of 5-Nitro-1,2,3-2*H*-triazole – High Performance Energetic Materials," *Journal of Materials Chemistry A*, 2013, **1**, 585–593 was the first University of Idaho publication. Now ten years and 36 JMCA publications later, a paper entitled "radical-mediated C–N bond activation in 3,5-diamino-4-nitro-1*H*-pyrazole towards high-energy and insensitive energetic materials," *Journal of Materials Chemistry A*, 2022, **10**, 8268–8272 was published. Coupling knowledge from various fields with a primary focus on materials for energy, including materials for energy storage and conversion, conservation of scarce natural resources, and sustainability and green processes, the journal was able to attract the best science resulting in a surging publication pressure leading to a rapidly increasing impact factor. The willingness to respond rapidly to an expanding area demand bodes well for many additional decades of successful science reporting.

Introduction

The development of highly thermostable and insensitive energetic materials (EMs) is driven by their possible applications in civilian industry, deep mines, and space exploration.[1–3] High nitrogen compounds have undergone rapid development as a class of energetic materials with high temperature resistance and safety within the past two decades.[4,5] 1*H*-Tetrazole is among the most sought after five-membered heterocycle in the field of EMs owing to its high nitrogen content, thermal stability, and energetic performance.[6] This heterocycle can endure harsh corrosive conditions (highly acidic and highly basic) and can be obtained readily in a single step by the addition of sodium azide to nitriles.[7] High-energy-density materials (HEDMs), based on the tetrazole ring, are environmentally friendly because they release nontoxic nitrogen gas upon decomposition.[8] Several research groups have demonstrated the importance of tetrazole compounds in achieving a good balance between energy density and stability.[9,10] However, pushing tetrazole compounds towards high detonation power is a challenging task[11] because the structural diversity of tetrazole compounds is largely limited by having only a single carbon available for functionalization.[12] Nevertheless, significant efforts have been made to obtain tetrazole compounds with excellent overall properties. Notable examples include the state-of the art secondary energetic TKX-50.[13,14]

Less appreciated, but with high potential as EMs, compounds which contain the oxime moiety are important precursors for the syntheses of HEDMs.[15] Dehydrative

[a]Department of Chemistry, University of Idaho, Moscow, Idaho, 83844-2343, USA. E-mail: jshreeve@uidaho.edu

[b]Department of Chemistry, Michigan State University, East Lansing, Michigan 48824, USA
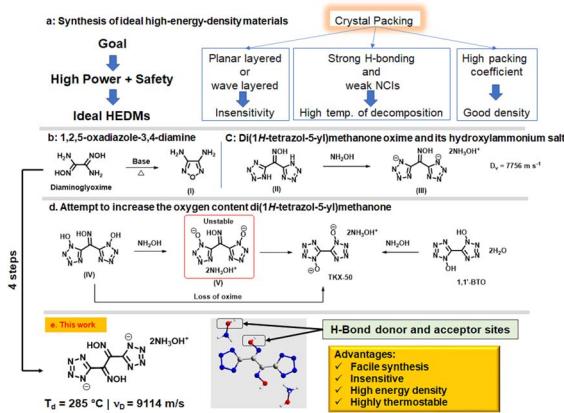
Fig. 1 (a) A longstanding goal of EMs. (b) Dehydrative cyclization of diaminoglyoxime. (c) A monoxime bistetrazole derivative and its dihydroxylammonium salt. (d) Examples of oxygen balance improving efforts on a mono oxime compound. (e) This work.

cyclization of a 1,2-dioxime to a furazan and oxidative cyclization of a 1,2-dioxime to a furoxan are two important strategies[16] in the syntheses of energetic materials with high enthalpies of formation and good densities (Fig. 1b). In spite of their favorable properties, oximes have been less explored as energetic materials. Previous attempts to prepare energetic salt derivatives of monoximes have led to the formation of a less energetic salt (III) or the loss of oxime itself (IV) (Fig. 1c and d).[15,17] Earlier studies of energetic salt formation with monoxime bistetrazole derivatives have shown that the oxime proton is less acidic relative to tetrazole and tetrazole N-oxide protons.[15] It was envisioned that H-bond interactions might be maximized using more stable dioximes in combination with a cation having donor–acceptor H-bond sites. More importantly, recent

extensive efforts have been made to utilize simple and easily available precursors for further functionalization and tuning of the properties to achieve high energy and low sensitivity.

In this work, new thermostable and insensitive high-energy compounds, 1,2-di(1H-tetrazol-5-yl)ethane-1,2-dione dioxime (**2**) and dihydroxylammonium 1,2-di(1H-tetrazol-5-yl)ethane-1,2-dione, (**3**), which contain dioximes with donor–acceptor H-bond sites, were synthesized from glyoxal (40% in water) in straightforward steps.

Results and discussion

Compound **1** can be prepared in three steps from glyoxal (40% in water).[18] The reaction of **1** with sodium azide in the presence of zinc bromide in aqueous solution results in the formation of 1,2-di(1H-tetrazol-5-yl)ethane-1,2-dione dioxime (**2**) (Scheme 1). The presence of an oxygen atom in the hydroxylammonium cation facilitates intermolecular H-bonding with the dianion. Dihydroxylamine 1,2-di(1H-tetrazol-5-yl)ethane-1,2-dione (**3**) was synthesized by reacting **2** with hydroxylamine (50% in H_2O). Compound **2** was also reacted with aqueous ammonia and 7H-[1,2,4]triazolo[4,3-b][1,2,4]triazole-3,6,7-triamine in acetonitrile to prepare energetic salts **4** and **5** (Scheme 1). The synthesis of the geminal nitro compound, 1,2-dinitro-1,2-di(1H-tetrazol-5-yl)ethane (**6a**), was attempted through the nitration of compound **2**. However, the reaction resulted in the formation of the cyclized (oxidative) product 3,4-di(1H-tetrazol-5-yl)-1,2,5-oxadiazole 2-oxide (**6**) (Scheme 1). In contrast, the nitration of the mono oxime derivative (**7**) under the *same* reaction conditions resulted in the isolation of the geminal nitro compound (**8**).[19] The attempted dehydrative cyclization of compound **2** to produce the furazan bistetrazole derivative in a highly basic reaction medium (aqueous NaOH), followed by acidification, resulted in compound **9** quantitatively (Scheme 1).
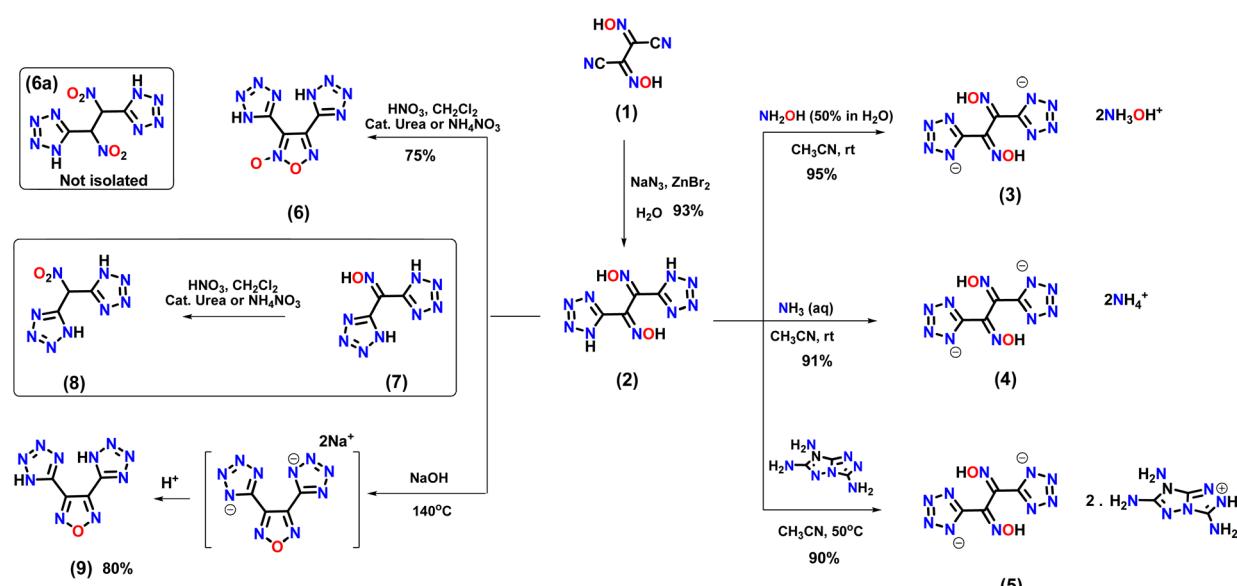
Scheme 1 . Synthesis of 1,2-di(1H-tetrazol-5-yl)ethane-1,2-dione dioxime (**2**), energetic salts (**3**–**5**), and cyclization reactions.

This journal is © The Royal Society of Chemistry 2023

*J. Mater. Chem. A*, 2023, **11**, 12896–12901 | **12897**
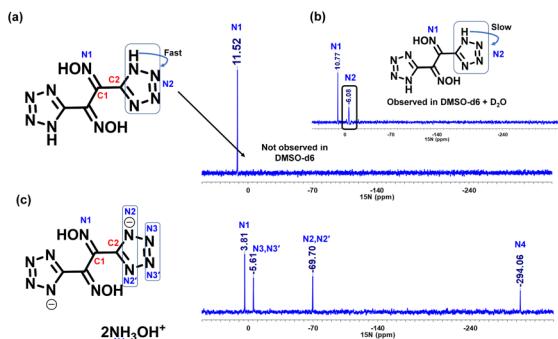
Fig. 2 ^{15}N NMR spectra of (a and b) compound **2**, (c) compound **3**.

In the ^{13}C NMR of compound **2**, two peaks, C1 and C2, were observed at 139.5 ppm and 146.1 ppm. In the nitrogen salts **3**, **4** and **5**, these two carbon peaks were shifted downfield and appear in the range of C1 at 142.2–143.4 ppm and C2 at 153.7–155.8 ppm, respectively. The ^{13}C NMR of compound **6** has four signals at δ 148.6, 145.8, 145.6, and 106.4. The conversion of dioxime (**2**) to furazan (**9**) was monitored by recording the changing shifts of the ^{13}C NMR signals. Upon cyclization, the C1 and C2 carbon peaks shifted downfield with resonances at 144.1 ppm and 147.6 ppm, respectively. Since all of the compounds are rich in nitrogen, the ^{15}N NMR spectra were recorded and compared. In DMSO-d6, compound **2** had only one signal at δ 11.5 (Fig. 2a). This arises from the fast exchange of protons between nitrogen atoms; therefore, the ^{15}N-NMR was recorded in a mixture of DMSO-d6 and D$_2$O. The second signal corresponding to N2 appears at δ −6.1 (Fig. 2b). Two signals (N1 and N2) for compound **2** are also observed upon increasing the concentration to saturation level in DMSO at δ −10.9 and δ −5.6, respectively. The ^{15}N NMR spectra of the dihydroxylammonium salt **3** has four signals. The signal for the oxime nitrogen (N1) was observed upfield (δ 3.8) in comparison to compound **2** (δ 10.8). The tetrazole ring nitrogen signals were observed at δ −69.7 (N2 and N2') and δ −5.6 (N3 and N3') (Fig. 2c).

The dihydroxylammonium salt **3** crystallizes in the $P2_1/n$ space group. In the crystal structure, the two oxime groups are found to be coplanar (plane 1), while the two tetrazole rings are in different planes (Fig. 3b). The torsion angles are O1–N1–C1–C2 = −0.9(2) and N1–C1–C2–N5 = −132.52(2), respectively. At 100 K, the calculated density for compound **3** is 1.838 g cm^{-3} and the packing coefficient is calculated to be 78.4%. The good crystal density of **3** is attributed to the presence of intermolecular hydrogen bonding between the hydroxylammonium cation and the dianion. The shortest H-bond is 1.64 Å. To better understand the relationship between molecular structures and their physical characteristics, Hirshfeld surfaces and 2D fingerprints were examined.[20,21] For compound **3**, four spikes were observed in the 2D fingerprint plot, which signifies O···H/H···O and N···H/H···N hydrogen bond interactions. The total amount of H-bond interactions, O–H···N and N–H···N, is 73.7% (Fig. 3d and e). The larger value of these stabilizing interactions enhances molecular stability and insensitivity of **3**. In the 2D fingerprint plot, the percentage of N···N and N···C interaction is
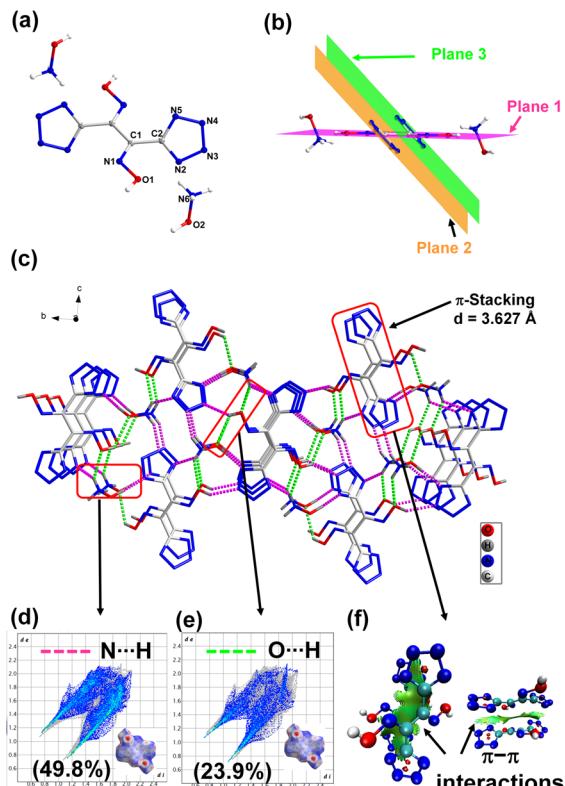

Fig. 3 (a) Labeling scheme of compound **3**. (b and c) Packing diagram and intermolecular interaction in **3**. (d and e) 2D fingerprint plots and Hirshfeld surfaces. (f) NCI plots.

14.2%, which indicates face-to-face π–π stacking. The π-stacking between molecules is also observed in the crystal structure with a distance of 3.627 Å. Since π-stacking interactions play an important role in reducing the sensitivity towards friction, the occurrence of these interactions between the molecules was further visualized by drawing NCIs plots.[22–24] As shown in Fig. 3f, wide green region isosurfaces between the parallel tetrazole rings implies face-to-face π–π interactions caused by π-stacking which contribute to the efficient packing (density) and insensitivity.
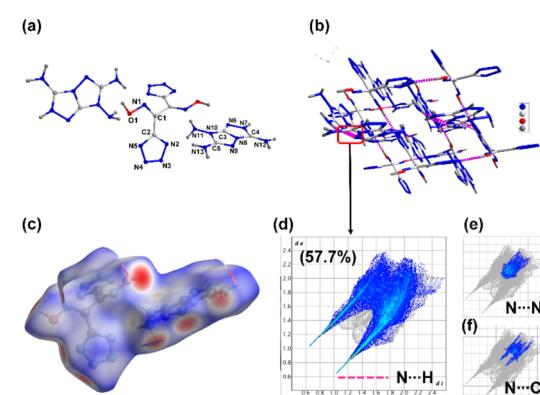
Fig. 4 (a) Labeling scheme of compound **5**. (b) Packing diagram and intermolecular interactions in compound **5**. (c–f) Hirshfeld surfaces and 2D fingerprint plots.

12898 | *J. Mater. Chem. A*, 2023, **11**, 12896–12901

This journal is © The Royal Society of Chemistry 2023

Compound **5** crystallizes in the monoclinic space group $C2/c$ with eight formula units per unit cell. In the crystal structure, the dianion exhibits a non-planar tetrahedral type of structure (Fig. 4a). The calculated crystal density for compound **5** is 1.748 g cm^{-3} at 100 K. The low density is attributed to the non-planar anion and lower packing coefficient (74.5%). Nevertheless, the packing diagram and 2D fingerprint plots show the weak but pivotal N···H/H···N hydrogen bond interactions and π-stacking interactions (Fig. 4c–f). In the 2D fingerprint plot of compound, two spikes related to N···H/H···N hydrogen bond interactions were observed. The relatively large percentage of N–H interactions (57.7%) gives rise to good thermal stability for compound **5** (Fig. 4d). The percentage of N···N and N···C interactions is 18.8%, which indicates the presence of π–π stacking between the rings.

Compound **6** crystallizes in the orthorhombic space group $P2_12_12_1$ with four chemical formula units per unit cell (Fig. 5). The calculated crystal density for compound **6** is 1.803 g cm^{-3} at 100 K. The relatively high density is attributed to the presence of intermolecular H-bonds and other weak non-covalent interactions. In the 2D fingerprint plot of compound **6**, the O···H/H···O and N···H/H···N hydrogen bond interactions are 12.3% and 18.4%, respectively (Fig. 5c and d). The percentage of N···C, N··N, and N···O interactions are 19.5, 22.7, and 25.8%, respectively, which suggests face-to-face π-stacking interactions between the planar five-membered rings (Fig. 5e–g). The isosurfaces between the furoxan and tetrazole rings were visualized by drawing a NCI plot (Fig. 5h). These interactions give rise to good temperature resistance and insensitivity to external stimuli.

High temperature resistance and insensitivity to external stimuli which are two highly important properties were determined using DSC and TGA analysis. Upon heating at 5 °C min^{-1}, the decomposition of **2** occurred at 281 °C (onset) and 289 °C (peak) (Fig. 6a and b). The dihydroxylammonium salt has a high thermal stability decomposing at 285 °C (onset) and 286 °C (peak) in the DSC and a sharp decomposition in TGA was observed at 281 °C (Fig. 6c and d). The diammonium salt **4** exhibits the highest decomposition temperature at 291 °C (onset) and 300 °C (peak); however, an endothermic peak at around 175 °C in the DSC and weight loss in the TGA was also observed (Fig. 6e and f). The decomposition of compound **5** occurs at 238 °C (onset) and 240 °C (peak) (Fig. 6g and h).

For compounds **2**, **3** and **4**, sensitivities to impact and friction were measured by using BAM standard methods,[25,26] and are given in Table 1. These compounds show very low sensitivity towards impact (>40 J) and friction (>360 J). The low sensitivity of compound **3** is further explained from both crystal structure and at the molecular level. Compound **3** has a wave-like packing pattern in the crystal structure (Fig. 7a), which when subjected to external stimuli can transform the mechanical energy into relative motion between layers. The impact sensitivity for compound **3** was measured at 60 J. At 60 J, compound **3** pressed into a pellet, which demonstrates that it is highly insensitive toward impact. At the molecular level, sensitivities of materials
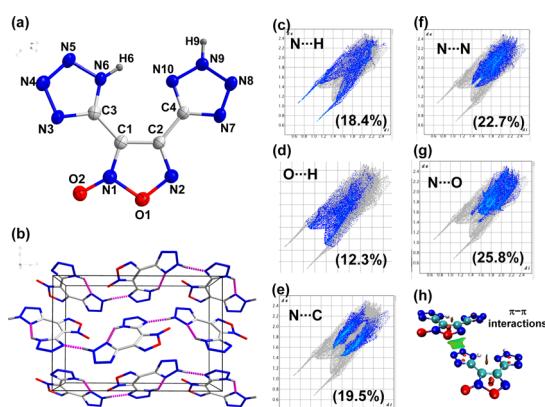
**Fig. 5** (a) Labeling scheme of compound **6**. (b) Packing diagram and intermolecular interaction in **6**. (c–g) 2D fingerprint plots (h) NCI plots.
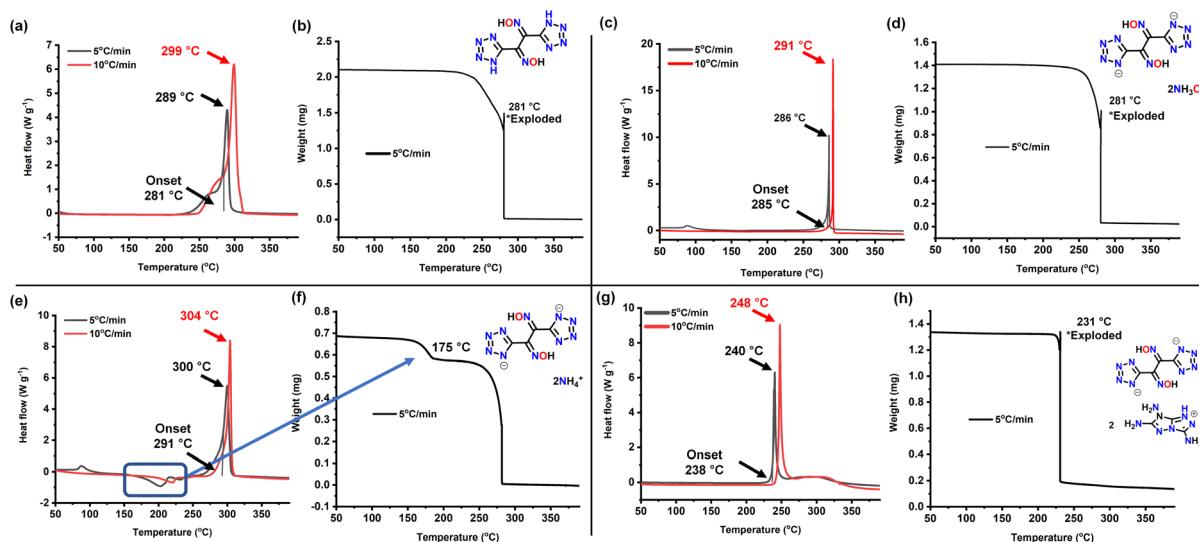
Fig. 6 DSC and TGA analysis of (a and b) compound **2**. (c and d) Compound **3**. (e and f) Compound **4**. (g and h) Compound **5**.

This journal is © The Royal Society of Chemistry 2023

J. Mater. Chem. A, 2023, **11**, 12896–12901 | **12899**

Table 1 Physicochemical properties of compounds **2**, **3** and **5**

	$T_d{}^a$ (°C)	ρ^b (g cm^{-3})	$\Delta H_f{}^d$ (kJmol^{-1})/kJg^{-1}	P^e (GPa)	$D_v{}^f$ (m s^{-1})<	IS^g (J)	FS^h (N)
2	281	1.85	666.1/2.97	29.3	8712	>40	>360
3	285	1.80/1.84^c	495.8/1.71	31.8	9114	>60	>360
5	239	1.75/1.80^c	1632.3/3.07	26.3	8545	>40	>360
II^i	288	1.74	590.5/2.90	27.4	8226	>40	—
III^i	260	1.60	669.5/2.44	17.8	7756	40	—
RDX^j	204	1.80	92.6/0.42	34.9	8795	7.5	120

^{a} Temperature (onset) of decomposition. ^{b} Density at 25 °C using gas pycnometer. ^{c} Density (calculated) - 100 K. ^{d} Molar enthalpy of formation calculated using isodesmic reactions with the Gaussian 03 suite of programs (revision D.01). ^{e} Pressure. ^{f} Velocity (calculated using EXPLO5 version 6.06.02). ^{g} Sensitivity to impact (IS). ^{h} Sensitivity to friction (FS). ^{i} Fig. 1 (compounds **II** and **III**). ^{j} ref. 27. All compounds were anhydrous powders for determination of properties in Table 1.
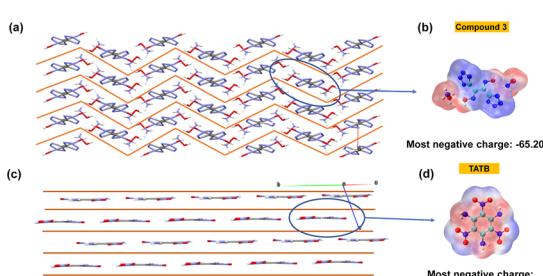

Fig. 7 (a) Wave-like layered packing of **3**; (b) ESP-mapped molecular surface of **3**; (c) planar packing of TATB; (d) ESP-mapped molecular surface of TATB.

toward impact are very much related to their electrostatic surface potentials (ESPs).

The electrostatic potentials (ESP) of compound **3** and TATB (for comparison) were calculated based on the B3LYP/6-311G(d, p) method with optimized structures. The calculated ESPs mapped surfaces of **3** and TATB are shown in Fig. 7b and d. It is seen that for compound **3**, the positive ESPs concentrate on the hydroxylammonium cation, while the negative ESPs distribute on the anion. The most negative ESP value in compound **3** is −65.20, lower than those in TATB (−27.58).

Densities at 25 °C (measured using a gas pycnometer) are 1.85 (**2**), 1.80 (**3**), and 1.75 (**5**) g cm^{-1}, respectively (Table 1). The enthalpies of formation (ΔH_f) for compounds **2–5** are given in Table 1. The calculated enthalpy of formation for compound **2** is 666.1 kJ mol^{-1}. Energetic salts **3** and **5** also have positive enthalpies of formation of 495.8 kJ mol^{-1} and 1632.3 kJ mol^{-1}, respectively. With experimental densities and calculated enthalpies of formation, detonation properties of compounds **2**, **3** and **5** were calculated using EXPLO5 (v6.06.02).[28] The calculated detonation velocities are 8712 (**2**), 9114 (**3**) and 8545 (**5**) m s^{-1}, and detonation pressures are 29.3 (**2**), 31.8 (**3**) and 26.3 (**5**) GPa, respectively.

For compounds **2–5**, the energetic behavior was determined by employing a red hot needle test. In this test, a glowing red-hot needle touched a 15 mg taped sample. Tests for compounds **2** and **3** show sharp deflagrations. As seen in Fig. 8a and b, they produce no smoke, whereas compounds **4** and **5** show no detonation and produce smoke upon burning (Fig. 8c and d). Practically, EMs are frequently used in combination with other EMs and non-EMs in energetic formulations. Therefore, the compatibility of a promising new EM is an important factor. Compound **3** was mixed in 1 : 1 ratio with TNT, RDX and TKX-50, and the temperatures of decomposition were determined using DSC measurements at the heating rate 10 °C min^{-1}. The DSC diagram of compound **3** at 10 °C min^{-1} is given in Fig. 8e. The mixtures show very slight differences from the decomposition temperature of the pure substance (Fig. 8f–h), which suggests that the compound **3** has good compatibility with TNT, RDX and TKX-50 and could be compatible for use in energetic formulations.

Conclusions

Unusual thermostable and insensitive high-energy compounds, 1,2-di(1H-tetrazol-5-yl)ethane-1,2-dione dioxime (**2**) and dihydroxylammonium 1,2-di(1H-tetrazol-5-yl)ethane-1,2-dione, (**3**) were synthesized in straightforward steps from glyoxal (40% in water). Compound **3** exhibits extensive donor–acceptor H-bonds and wave-like crystal packing, which provides good thermostability and insensitivity. It also has good density, and a high heat of formation which contribute to its high detonation performance. Additionally, it shows good compatibility with other energetics which makes it attractive as a potentially new high-energy-density material for practical use.


Fig. 8 (a–d) Hot needle tests of compounds **2–5**. (e) DSC analysis of **3** at heating rate 10 °C min^{-1} (f) DSC analysis of **3**:TNT (1 : 1) (g) DSC analysis of **3**:RDX (1 : 1) (h) DSC analysis of **3**:TKX-50 (1 : 1).

Conflicts of interest

There are no conflicts to declare.

12900 | *J. Mater. Chem. A*, 2023, **11**, 12896–12901

This journal is © The Royal Society of Chemistry 2023

Acknowledgements

References

1 T. M. Klapötke, *High Energy Density Materials*, Springer, Berlin, 2012.

2 J. P. Agrawal, *High Energy Materials*, Wiley, 2010.

3 J. Zhang, Y. Feng, Y. Bo, R. J. Staples, J. Zhang and J. M. Shreeve, *J. Am. Chem. Soc.*, 2021, **143**, 12665–12674.

4 M. Göbel, K. Karaghiosoff, T. M. Klapötke, D. G. Piercey and J. Stierstorfer, *J. Am. Chem. Soc.*, 2010, **132**, 17216–17226.

5 L. Hu, P. Yin, G. Zhao, C. He, G. H. Imler, D. A. Parrish, H. Gao and J. M. Shreeve, *J. Am. Chem. Soc.*, 2018, **140**, 15001–15007.

6 B. Wang, X. Qi, W. Zhang, K. Wang, W. Li and Q. Zhang, *J. Mater. Chem. A*, 2017, **5**, 20867–20873.

7 F. R. Benson, *Chem. Rev.*, 1947, **41**, 1–61.

8 M. Benz, T. M. Klapötke, J. Stierstorfer and M. Voggenreiter, *J. Am. Chem. Soc.*, 2022, **144**, 6143–6147.

9 T. M. Klapötke and J. Stierstorfer, *Green Energetic Materials*, ed. T. Brinck, Wiley, Hoboken, NJ, 2014, pp. 133–178.

10 M. H. H. Wurzenberger, M. Lommel, M. S. Gruhne, N. Szimhardt and J. Stierstorfer, *Angew. Chem., Int. Ed.*, 2020, **59**, 12367–12370.

11 Q. Yu, G. H. Imler, D. A. Parrish and J. M. Shreeve, *Org. Lett.*, 2019, **21**, 4684–4688.

12 R. Haiges and K. O. Christe, *Inorg. Chem.*, 2013, **52**, 7249–7260.

13 T. M. Klapötke and M. Suceska, *Z. Anorg. Allg. Chem.*, 2021, **647**, 572–574.

14 N. Fischer, D. Fischer, T. M. Klapötke, D. G. Piercey and J. Stierstorfer, *J. Mater. Chem.*, 2012, **22**, 20418.

15 D. Chand, D. A. Parrish and J. M. Shreeve, *J. Mater. Chem. A*, 2013, **1**, 15383–15389.

16 R. A. Olofson and J. S. Michelman, *J. Am. Chem. Soc.*, 1964, **86**, 1863–1865.

17 G. Zhao, C. He, P. Yin, G. H. Imler, D. A. Parrish and J. M. Shreeve, *J. Am. Chem. Soc.*, 2018, **140**, 3560–3563.

18 D. Fischer, T. M. Klapötke, M. Reymann and J. Stierstorfer, *Chem. – Eur. J.*, 2014, **20**, 6401–6411.

19 G. Zhao, C. He, H. Gao, G. H. Imler, D. A. Parrish and J. M. Shreeve, *New J. Chem.*, 2018, **42**, 16162–16166.

20 M. A. Spackman and J. J. McKinnon, *CrystEngComm*, 2002, **4**, 378–392.

21 M. A. Spackman and D. Jayatilaka, *CrystEngComm*, 2009, **11**, 19–32.

22 T. Lu and F. Chen, *J. Comput. Chem.*, 2012, **33**, 580–592.

23 E. R. Johnson, S. Keinan, P. Mori-Sánchez, J. Contreras-García, A. J. Cohen and W. Yang, *J. Am. Chem. Soc.*, 2010, **132**, 6498–6506.

24 W. Humphrey, A. Dalke and K. Schulten, *J. Mol. Graph.*, 1996, **14**, 33–38.

25 NATO, Standardization Agreement 4489 (STANAG4489), Explosives, Impact Sensitivity Tests 1999.

26 NATO, Standardization Agreement 4487 (STANAG 4487), Explosives, Friction Sensitivity Tests 2002.

27 Y. Tang, C. He, L. A. Mitchell, D. A. Parrish and J. M. Shreeve, *J. Mater. Chem. A*, 2016, **4**, 3879–3885.

28 M. Sućeska, *EXPLO5 6.01*, Brodarski Institute, Zagreb, Croatia, 2013.

This journal is © The Royal Society of Chemistry 2023

J. Mater. Chem. A, 2023, **11**, 12896–12901 | **12901**